Journal of Materials Chemistry B

Crystalline H-Aggregate Nanoparticles for Detecting Dopamine Release from M17 Human Neuroblastoma Cells

Journal:	*Journal of Materials Chemistry B*
Manuscript ID	TB-ART-07-2022-001450.R2
Article Type:	Paper
Date Submitted by the Author:	27-Aug-2022
Complete List of Authors:	Reddy, Nitin; University of Central Florida, Advanced Materials Processing and Analysis Dicce , Arianna ; University of Central Florida, Advanced Materials Processing and Analysis ma, yiping; University of Central Florida, Advanced Materials Processing and Analysis Center Chen, Limei ; University of Central Florida, Burnett School of Biomedical Sciences Chai, Karl; University of Central Florida, Burnett School of Biomedical Sciences Fang, Jiyu; University of Central Florida, Advanced Materials Processing and Analysis Center

Crystalline H-Aggregate Nanoparticles for Detecting Dopamine Release from M17 Human Neuroblastoma Cells

Nitin Ramesh Reddy,[1] Arianna Dicce,[1] Yiping Ma,[1] Li-Mei Chen,[2] Karl X. Chai,*,[2] and Jiyu Fang*,[1]

[1]Department of Materials Science and Engineering and Advanced Materials Processing and Analysis Center, [2]Division of Cancer Research, Burnett School of Biomedical Sciences, College of Medicine, University of Central Florida, Orlando, Florida 32816
*Email: Jiyu.Fang@ucf.edu; Email: Xinqing.Chai@ucf.edu

Abstract

Dopamine (DA) is an important neurotransmitter, which is essential for transmitting signals in neuronal communications. The deficiency of DA release from neurons is implicated in neurological disorders. There has been great interest in developing new optical probes for monitoring the release behavior of DA from neurons. H-aggregates of organic dyes represent an ordered supramolecular structure with delocalized excitons. In this paper, we use the self-assembly of 3,3'-diethylthiadicarbocyanine iodide ($DiSC_2(5)$) in ammonia solution to develop crystalline H-aggregate nanoparticles, in which $DiSC_2(5)$ molecules show a long-range π-π stacking. The crystalline H-aggregate nanoparticles are stable in cell culture medium and can serve as an efficient photo-induced electron transfer (PET) probe for the detection of DA with the concentration as low as 0.1 nM in cell culture medium. Furthermore, the crystalline H-aggregate nanoparticle-based PET probe is used to detect the release behavior of DA from the M17 human neuroblastoma cells. We find that the DA release from the cells is enhanced by nicotine stimulations. Our results highlight the potential of crystalline H-aggregate nanoparticle-based PET probe for diagnosing nervous system diseases and verifying therapies.

Keywords: H-aggregate nanoparticles, photo-induced electron transfer, detection, dopamine release, cells, nicotine stimulations.

1. Introduction

Dopamine (DA) is a catecholamine neurotransmitter that plays a vital role in transmitting signals in synaptic communication between cells.[1] The deficiency of DA release from cells has implications in the pathophysiology of neurological disorders, including Parkinson's[2-3] and Alzheimer's diseases.[4-5] Given the physiological importance of DA, there has been interested in developing new analytical methods for studying the release behavior of DA from cells with the goal of understanding of DA regulations and diagnosing neurological disorders. Electrochemical measurements are commonly used for the detection of DA. Since that the concentration of DA released cells is very low,[6] great efforts have been made in designing electrode materials by using carbon fibers,[7] carbon nanotubes,[8-9] carbon particles,[10] and carbon nanosheets[11] for improving the sensitivity of electrochemical methods in the detection of DA release from cells. In comparison with electrochemical methods, optical probes have advantages including high sensitivity, small size, cost effectiveness and simple operation. Recently, the plasmon absorbance of Au nanoparticles[12-13] and fluorescence of quantum dots[14-16] have been used as optical probes for the simple, rapid and sensitive detection of DA in aqueous solution.

Photoinduced electron transfer (PET) is often used in the design of colorimetric and fluorometric optical probes, in which the PET efficiency is a key for achieving the high sensitivity of the probes in the detection of analytes.[17] H- and J-aggregates of organic dyes represent highly ordered supramolecular structures. Due to their delocalized excitons, the PET of H- and J-aggregates are highly efficient.[18-20] Thus, they may serve as highly efficient PET probes for the detection of DA. It is known that H- and J-aggregates show distinctly different photophysical properties in absorption, fluorescence, and excited state lifttime. According to the Kasha's excitonic theory, the electronic excited state of J- and H-aggregates splits due to the strong

coupling of organic dyes. For J-aggregates, the allowed energy transition is from the ground state to the lower excited state, leading to a red-shifted J-band with respect to the monomer band and a nearly resonant fluorescence emission. While for H-aggregates, the allowed energy transition is from the ground state to the higher excited state, giving a blue-shifted H-band. The fluorescence emission of H-aggregates is largely quenched due to the rapid relaxation of the excited energy from the higher excited state to the forbidden lower excited state.

Recently, J-aggregate nanotubes from the co-assembly of 3,3'-diethythiadicarbocyanine iodide ($DiSC_2(5)$) and lithocholic acid (LCA) were developed as a PET probe for the detection of DA in synthetic urine.[21-22] The detection limit of the J-aggregate nanotube-based PET probe for DA was estimated to be ~ 7 nM.[21] It was reported that the photoinduced electron generation[23-24] and excited state lifetime [25-26] of H-aggregates were greater than those of J-aggregates, suggesting that H-aggregates may serve as a highly sensitive PET probe for the detection of DA. It is known that H- and J-aggregates of organic dyes are formed through noncovalent interactions such as electrostatic, hydrophobic and π-π interactions. Thus, one of the major challenges of using H- and J-aggregates as efficient PET probes is their stability in biological fluids. In this paper, we form crystalline H-aggregate nanoparticles by the self-assembly of $DiSC_2(5)$ in ammonia solution. The structure and optical properties of crystalline H-aggregate nanoparticles are studied. We show that the crystalline nanoparticles are stable and can be used as a highly efficient PET probe for the sensitive detection of DA in synthetic urine and cell culture medium. The detection limit of the crystalline H-aggregate nanoparticles for DA in synthetic urine is twice lower than that of the J-aggregate nanotubes. In cell culture medium, the crystalline H-aggregate nanoparticles are able to response to DA with the concentration as low as 0.1 nM, which is lower than the detection limit of Au nanoparticles[12-13] and quantum dots.[14-16] Due to their good stability and high sensitivity, the crystalline H-aggregate

nanoparticles is used as PET probe for detecting the release behavior of DA from M17 human neuroblastoma cells with/without nicotine stimulations.

2. Experimental

Materials: 3,3'-diethylthiadicarbocyanine iodide ($DiSC_2(5)$), dopamine (DA), ascorbic acid (AA), uric acid (UA), and nicotine were procured from Sigma Aldrich and used without further purification. 30% ammonia solution was from Sigma-Aldrich. De-ionized (DI) water was obtained from an Easypure II system (18 MΩ cm, pH 5.7). Synthetic urine (97.17 wt% water, 1.9 wt% urea, 0.77 wt% sodium chloride, 0.09 wt% magnesium sulfate heptahydrate, 0.06 wt% calcium chloride dihydrate) was from Ricca chemical company. The synthetic urine was diluted by 10 times with DI water before being used. OPTI-MEM (a reduced serum medium with insulin, transferrin, hypoxanthine, thymidine, and trance) was from Invitrogen. Holey Formvar filmed grids were purchased from Electron Microscopy Science.

Preparation and characterization of crystalline H-aggregate nanoparticles: 1 mM $DiSC_2(5)$ was dissolved in 30% ammonium solution with pH 13.0 in a glass vial. The solution was heated in an ultrasonic bath (Branson 1510, Branson Ultrasonics Co.) at 55°C for 10 min and then cooled down to room temperature. The formation of crystalline H-aggregates nanoparticles was observed after the $DiSC_2(5)$ solution was aged for 72 h. After the formation of crystalline H-aggregate nanoparticles, ammonia was allowed to evaporate from open vials for overnight. The supernatant of crystalline H-aggregate nanoparticle solution was collected and characterized. Absorption spectra were taken with Agilent Cary 60 UV-vis spectrophotometer. For the measurement of temperature-dependent absorption spectra, the supernatant of crystalline H-aggregate nanoparticle solution was placed in a glass cuvette on a thermoelectric stage (Instec TS62 with an STC 200 temperature controller). The supernatant solution was allowed to stabilize for 10 min after each temperature increment before the UV-vis absorption spectra were recorded. Fluorescence spectra

were taken at the synchronous mode with Δ = 40 nm using Jasco FP-6500 spectrofluorometer. For transmission electron microscopes (TEM) measurements, the supernatant solution of crystalline H-aggregate nanoparticles was dried on Holey Formvar filmed grids. Low-resolution TEM images were taken with JEOL JEM-1011 at an accelerating voltage of 100 kV. High-resolution TEM images were recorded with Tecnai F30 at an accelerating voltage of 200 kV. Cyclic voltammetry (CV) measurements were conducted in an aqueous solution with 1 M KCl using a CHI 627C Electrochemical workstation. The supernatant solution of crystalline H-aggregate nanoparticles was drop-casted on an ITO working electrode, a platinum wire and Ag/AgCl were used as a counter electrode and reference electrode, respectively. The CV scan was performed from − 0.3 to 1 V at a scanning rate of 0.01 V/s.

Detection of dopamine in synthetic urine and culture medium: 1 mL of the supernatant solution of crystalline H-aggregate nanoparticles was added to 1mL synthetic urine and OPTI-MEM I (a reduced serum medium), followed by the addition of DA with different concentrations. After 240 min incubation, the UV-vis absorption spectra of crystalline H-aggregate nanoparticles in the diluted synthetic urine and culture medium were recorded.

Detection of dopamine released from Cells: M17 human neuroblastoma cells were maintained in OPTI-MEM medium. A total of 4×10^5 cells/well was then seeded into a 12-well plate (Corning Inc., Kennebunk, ME) and cultured overnight in a humidified incubator at 37 °C with 5% CO_2. A colorimetric Universal Dopamine ELISA Kit (Novus Biologicals, Centennial, CO) was used to quantitate the DA released in the medium from cultured M17 cells. The culture medium (5 ml in volume) from a confluent culture of 2.2×10^6 cells in a T-25 tissue culture flask (Sarstedt, Newton, NC) following a 72-hour incubation was recovered and centrifuged at 16,300 × g for 10 min to remove cell debris. The amount of DA released in the culture medium was determined by

colorimetric Universal Dopamine ELISA Kit to be ~ 0.3 nM. Phase contrast microscopy images of M17 cells was captured with a Nikon D3500 DSLR camera, mounted atop a Nikon Eclipse E600 upright microscope. On the second day after M17 cells were cultured into a 12-well plate, nicotine with different concentrations was added to the culture medium to stimulate the release of DA from the M17 cells. After 24 h of incubation, the medium was collected and centrifuged at 16,300 × g for 10 min to remove cell debris. 0.1 mL of the centrifuged medium was added in a cuvette, followed by the addition of 0.1 mL of the supernatant solution of crystalline H-aggregate nanoparticles.

3. **Results and Discussion**

$DiSC_2(5)$ is a cationic cyanine dye that consists of two heterocyclic nitrogen centers bridged by a π-conjugated polymethine chain (Fig. 1a). 1mM $DiSC_2(5)$ in methanol showed a monomer absorption band at 647 nm and a short-wavelength shoulder band at 580 nm (Fig. 1b). The shoulder band suggests the formation of $DiSC_2(5)$ dimers.[27] In a previous study, we showed that $DiSC_2$ (5) in 15% ammonia solution formed both H- and J-aggregates.[28] Interestingly, 1mM $DiSC_2(5)$ in 30% ammonia solution only formed H-aggregates with the H-band at 450 nm (Fig. 2b). The H-band was blue-shifted by 197 nm with respect to the monomer band. The largely blue-shifted H-band indicated that the strong coupling of $DiSC_2(5)$ molecules in H-aggregates. Ammonia is a weak base and gains protons from water to form ammonium ion (NH_4^+) and hydroxide ion (OH^-). The charge of cationic $DiSC_2(5)$ molecules in ammonia solution was likely screened by OH^- ions. Thus, the hydrophobic and π-π interactions of $DiSC_2(5)$ molecules were believed to be responsible for the formation of H-aggregates in ammonia solution. Low-resolution TEM images showed that the size of H-aggregates was in the range from 5 nm to 60 nm (Fig. 1c). High-resolution TEM images revealed that the H-aggregate nanoparticles had an ordered lamellar

structure with the spacing of ~ 0.34 nm (Fig. 1d), which matched the π-π stacked distance of cyanine dyes reported in the literature.[29-30] Thus, the lamellar structure shown in Fig. 1d represents a long-range π-π stacking of $DiSC_2(5)$ molecules in H-aggregate nanoparticles.

Fig. 2a shows the temperature-dependent absorption spectra of the supernatant solution of crystalline H-aggregate nanoparticles. The H-band intensity of crystalline H-aggregate nanoparticles at 450 nm gradually decreased with the increase of temperature, suggesting the weakening of the coupling of $DiSC_2(3)$ molecules. There was no monomer band observed with the increase of temperature from 20 °C to 65 °C. However, beyond 65 °C, the monomer band at 647 nm appeared and rapidly increased with the increase of temperature (Fig. 2b). This result indicated that the disassembly of crystalline H-aggregate nanoparticles started at 65 °C.

The structural integrity of crystalline H-aggregate nanoparticles in biological fluids is essential for sensing applications. Synthetic urine, which comprises urea, sodium chloride, calcium chloride dehydrate, and magnesium sulfate heptahydrate, was often used to mimic urine characteristics. Thus, the stability of H-aggregate nanoparticles in synthetic urine was studied. In our experiments, 1 mL of the supernatant solution of crystalline H-aggregate nanoparticles was added to 1 mL of synthetic urine. The pH of the diluted synthetic urine was ~ 11. The crystalline H-aggregate nanoparticles in the diluted synthetic urine showed negligible change in their absorption spectra over 150 min (Fig. 3a), suggesting that the chemicals in synthetic urine were unable to disrupt the long-range π-π stacking of $DiSC_2(5)$ molecules in the crystalline H-aggregate nanoparticles. After the addition of 1 μM DA, the H-band intensity of crystalline H-aggregate nanoparticles gradually decreased over time (Fig. 3b) and gradually leveled off after 240 min, in which the H-band intensity dropped by 34 % (Fig. 3c).

DA is redox active (Fig. 4a). It could be oxidized into quinone by ambient O_2 in aqueous solution when pH was higher than 7.0.[31] DA-quinone could serve as an electron acceptor.[32] Fig. 4b shows the UV-vis absorption spectra of 0.5 μM DA in water with pH 5.7 and the diluted synthetic urine with pH 11. The absorption band at ~ 280 nm was attributed to DA. While the absorption band at ~ 350 nm observed in the diluted synthetic urine was attributed to DA-quinone.[33] Since the fluorescence emission of the crystalline H-aggregate nanoparticles was largely quenched, Forster resonance energy transfer from crystalline H-aggregate nanoparticles to DA-quinone could be ruled out. It is known that the electron transfer from a donor to an acceptor depends on the relative position of their highest occupied molecular orbital (HOMO) and the lowest unoccupied molecular orbital (LUMO). The HOMO and LUMO levels of crystalline H-aggregate nanoparticles were estimated from their oxidation potential measured with cyclic voltammetry (CV) (Fig. 4c) and the optical band gap (E_g) measured by using the onset of their absorption spectra using the following equations:[34]

$$E_{HOMO} = -e\,(E_{onset} + 4.4) \quad (1)$$

$$E_{LUMO} = E_g + E_{HOMO} \quad (2)$$

The onset of oxidation (E_{onset}) for H-aggregate nanoparticles was measured from the CV curve to be 0.381 eV. Inputting the E_{onset} in equation (1), we calculated the E_{HOMO} to be - 4.781 eV. The E_g was calculated to be 3.34 eV using the equation $E_g = 1242/\lambda_{onset}$, where λ_{onset} is the onset of the H-band at 381 nm. Thus, the E_{LUMO} was found to be -1.531 eV from equation (2). It was reported that the LUMO level of DA-quinone was - 3.42 eV,[35] which was located between the E_{HOMO} and E_{LUMO} of crystalline H-aggregate nanoparticles (Fig. 4d). Thus, the photo-induced electron transfer (PET) from the excited state of the crystalline H-aggregate nanoparticles to the ground state of DA-quinone was allowed.

To further verify the PET mechanism, we measured the relative intensity change ($\Delta I/I_o$) of the H-band after the crystalline H-aggregate nanoparticles were incubated with 20 nM DA for 240 min in buffer solution with different pH values. Where $\Delta I = I_0 - I$. I_0 is the H-band intensity in the absence of DA, and I is the H-band intensity in the presence of DA. As can be seen in Figure 4a, DA should be in the reduced form at pH 5. In this case, we found that the $\Delta I/I_o$ was very small and negligible (Fig. 5). While DA should be oxidized into quinone in the buffer solution with pH 7 and 8, in which the $\Delta I/I_o$ largely increased (Fig. 5). This result further confirms that the PET from the excited state of the crystalline H-aggregate nanoparticles to the ground state of DA-quinone is responsive to the $\Delta I/I_o$ of the H-band.

For comparison with the J-aggregate nanotube-based PET probe reported in the literature,[21] we measured the UV-vis absorption spectral change of the crystalline H-aggregate nanoparticle-based PET probe in the diluted synthetic urine after the addition of DA in the same concentration range from 10 nM to 80 nM. In our experiments, each absorption spectra were taken after 240 min incubation. It was clear in Fig. 6a that the intensity of the H-band at 450 nm gradually decreased as the increase of DA concentrations. The plot of the $\Delta I/I_o$ of the H-band as a function of DA concentrations showed a linear relationship (Fig. 6b). The detection limit of the crystalline H-aggregate nanoparticles for DA in the diluted synthetic urine, which was determined by taking a ratio of the standard deviation and the slope obtained from the linear fit shown in Fig. 6b and then multiplying this value by 3.3, was ~ 3.4 nM, which was twice lower than that of the J-aggregate nanotubes. It was shown that the photoinduced electron generation [23] and excited state lifetime[25] of H-aggregates was greater than that of J-aggregates. In addition, we noted that the excited energy level of the crystalline H-aggregate nanoparticles shown in Fig.4d was higher than that of the J-aggregate nanotubes (-2.19 eV). The longer excited lifetime and higher excited energy level of the

H-aggregate nanoparticles might favor for the PET to DA-quinone and attribute to the lower detection limit, compared to the J-aggregate nanotubes.

Ascorbic acid (AA) and uric acid (UA) are considered as major interference species for the detection of DA. The UV-vis absorption spectra of crystalline H-aggregate nanoparticles in the diluted synthetic urine after the addition of AA and UA with the concentration from 10 nM to 80 nM are shown in Fig. 7a and 7b, respectively. The $\Delta I/I_o$ of the H-band at 450 nm in the presence of 80 nM UA and 80 nM AA was much smaller than that in the presence of 80 nM DA. It was reported that UA and AA could not easily be oxidized in aqueous solution with pH higher than 7.0.[36] Thus, the PET from crystalline H-aggregate nanoparticles to UA and AA was limited because the poorly oxidized UA and AA could not be served as electron acceptors in synthetic urine.

We would like to point that the J-aggregate nanotubes formed by the co-assembly of $DiSC_2(5)$ and LCA were unstable and gradually disassembled in the OPTI-MEM I medium of M17 human neuroblastoma cells. While the crystalline H-aggregate nanoparticles of $DiSC_2(5)$ were found to be stable in the OPTI-MEM I culture medium. In our experiments, 1 mL of the supernatant solution of crystalline H-aggregate nanoparticles was added to 1mL of the OPTI-MEM I culture medium. The pH of the diluted culture medium was 11.8, in which DA was oxidized into quinone. Fig. 8a shows the time-dependent UV-vis absorption spectra of crystalline H-aggregate nanoparticles in the diluted culture medium. The absorption band at 560 nm was from the culture medium. The intensity change of the H-band at 450 nm was negligible over time (Fig. 8b), suggesting that the crystalline H-aggregate nanoparticles were stable in the diluted culture medium. After the addition of 0.1 nM DA, the apparent decrease of the H-band intensity was observed over time (Fig. 9a). The DA concentration detected by crystalline H-aggregate

nanoparticles is lower than the detection limit of Au nanoparticles (0.5nM) [13], quantum dots (0.3 nM)[16], and electrochemical sensors (10 nM).[11] The decrease of the H-band intensity was gradually enlarged when the concentration of DA increased to 1nM (Fig. 9b) and 2 nM (Fig. 9c). For comparison, we plotted the $\Delta I/I_o$ of the H-band as a function of DA concentrations from 0.1 nM to 5 nM after 240 min incubation of crystalline H-aggregate nanoparticles with DA, which showed a near linear relationship (Fig. 9d). The high sensitivity of crystalline H-aggregate nanoparticles for DA is critical for detecting the DA released from cells because the level of the released DA is generally low.

Finally, we exploited the potential of crystalline H-aggregate nanoparticles for detecting the DA released in the OPTI-MEM I culture medium from the M17 human neuroblastoma cells, which were dopaminergic and capable of releasing DA.[37] In our experiments, the M17 cells were maintained in the OPTI-MEM I medium.[38] For the detection of DA release by using crystalline H-aggregate nanoparticles, M17 cells were seeded into a 12-well plate at 4×10^5 cells/well and cultured overnight in the OPTI-MEM I medium (Fig. 10a). The culture medium was then centrifuged for 10 min to remove cell debris. 0.1 mL of the supernatant solution of crystalline H-aggregate nanoparticles was then added in 0.2 mL of the centrifuged medium with the released DA. Fig. 10b shows the time-dependent absorption spectra of crystalline H-aggregate nanoparticles in the culture medium with the released DA. The $\Delta I/I_o$ of the H-band gradually increased over time and leveled off after 240 min (Fig. 10c). This result confirmed the ability of crystalline H-aggregate nanoparticles as a PET probe for the detection of the DA released in the culture medium from the M17 neuroblastoma cells.

Nicotine is a well-established neurotransmitter releasing agent, which is able to stimulate the release of DA from cells by activating the α7 nicotinic (acetylcholine) receptor (nAChR-α7)

expressed on the surface of cells.[39-40] In our experiments, nicotine with different concentrations was added in the OPTI-MEM I medium of M17 neuroblastoma cells cultured on the 12-well plate. After 24-hour incubation with nicotine, the culture medium was centrifuged for 10 min to remove cell debris. 0.1 mL of the supernatant solution of crystalline H-aggregate nanoparticles was then added in 0.2 mL of the centrifuged medium with the released DA. The time-dependent absorption spectra of crystalline H-aggregate nanoparticles in the culture medium with the released DA under 25 μM and 50 μM nicotine stimulations are shown Fig. 11a and 11b, respectively. The relative $\Delta I/I_o$ of the H-band at 450 nm after 240 min incubation with 0 μM, 25 μM and 50 μM nicotine was 0.17, 0.20 and 0.23, respectively (Fig. 11c). There was no further increase in the $\Delta I/I_o$ when the concentration of nicotine increased to 100 μM. The increase of the $\Delta I/I_o$ indicated that the release of DA from the M17 cells was enhanced by nicotine stimulations.

4. **Conclusions**

We have developed crystalline H-aggregate nanoparticles by the self-assembly of $DiSC_2(5)$, which shows a large, blue-shifted H-band with respect to the monomer band and a long-range π-π stacking of $DiSC_2(5)$ molecules. The crystalline H-aggregate nanoparticles are stable in synthetic urine and cell culture medium. The photo-induced electron transfer (PET) from the excited state of the crystalline H-aggregate nanoparticles to the ground state of DA-quinone leads to the decrease of the H-band intensity, providing a simple probe for the highly sensitive detection of DA in synthetic urine and culture medium. Due to their good stability and high sensitivity, the crystalline H-aggregate nanoparticles are used as a PET probe to detect the DA released in culture medium from M17 human neuroblastoma cells. We show that the release of DA from M17 cells is enhanced by nicotine stimulations. Our results highlight the potential of crystalline H-aggregate nanoparticles for diagnosing nervous system diseases and screening therapeutic agents.

Notes

The authors declare no competing financial interest.

ACKNOWLEDGMENTS

This work was supported by the US National Science Foundation (CBET 1803690).

References:

1. A. Roy and R. A. Wise, *Nat. Rev. Neurosic.* 2004, **5**, 483−494.
2. J. Lotharious and P. Brundin, *Nat. Rev. Neurosci*. 2002, **3**, 932−942.
3. C. Buddhala, S. K. Loftin, B. M. Kuley, N. J. Cairns, M. C. Campbell, J. S. Perlmutter and P. T. Kotzbauer, *Ann. Clin. Transl. Neurol*. 2015, **2**, 949−959.
4. D. J. Selkoe, *Science* 2002, **298**, 789–791.
5. X. F. Pan, A. C. Kaminga, S. W. Wen, X. Y. Wu, K. Acheampong and A. Z. Liu, *Front. Aging Neurosci*. 2019, **11**, 175.
6. K. Jackowsk and P. Krysinski, *Anal. Bioanal. Chem*. 2013, **405**, 3753– 3771.
7. A. V. Heien, A. S. Khan, J. L. Ariansen, J. F. Cheer, P. E. M. Phillips, K. M. Wassum and R. M. Wightman, *Proc. Natl. Acad. Sci. USA* 2005, **102***,* 10023–10028.
8. S. Krussa, D. P. Salema, L. Vukovi, B. Lima, E. V. Ende, E. S. Boydend and M. S. Stranoa, *Proc. Natl. Acad. Sci. U.S.A.* 2017, **114**, 1789–1794.
9. A. G. Beyene, K. Delevich, J. Travis, D. Bonis-O'Donnell, D. J. Piekarski, W. C. Lin, A. W. Thomas, S. J. Yang, P. Kosillo, D. Yang, G. S. Prounis, L. Wilbrecht and M. P. Landry, *Sci. Adv.* 2019, **5**, eaaw3108
10. N. Akhtar, M. Y. Emran, M. A. Shenashen, H. Khalifa, T. Osaka, A. Faheem, T. Homma, H. Kawarada and S. A. El-Safty. *J. Mater. Chem. B* 2017, **5**, 7985-7996.
11. M. A. Shenashen, H. Morita and S. A. El-Safty. *Adv. Healthcare Mater*. 2018, **7**, 1701459.
12. R. Baron, M. Zayats and I. Willner, *Anal. Chem.* 2005, **77**, 1566–1571.
13. B. Kong, A. Zhu, Y. Luo, Y. Tian, Y. Yu and G. Shi, *Angew. Chem. Int. Ed.* 2011, **50**, 1837–1840.

14. Y. L. Zhong, F. Peng, F. Bao, S. Y. Wang, X. Y. Ji, L. Yang, Y. Y. Su, S. T. Lee and Y. He, *J. Am. Chem. Soc*. 2013, **135**, 8350–8356.

15. Q. Mu, H. Xu, Y. Li, S. J. Ma and X. H. Zhong, *Analyst* 2014, **139**, 93– 98.

16. X. Zhang, X. Chen, S. Kai, H.-Y. Wang, J. Yang, F.-G Wu and Z. Chen, *Anal. Chem.* 2015, **87**, 3360–3365.

17. B. Daly, J. Ling and A. P. de Silva, *Chem. Soc. Rev.* 2015, **44**, 4203–4211.

18. T. L. Penner and D. Moebius, *J. Am. Chem. Soc.* 1982, **104**, 7407–7413.

19. K. Liang, K. Y. Law and D. G. Whitten, *J. Phys. Chem.* 1995, **99**, 16704–16708.

20. S. Das and P. V. Kamat, *J. Phys. Chem. B* 1999, **103**, 209– 215,

21. N. R. Reddy, S. Rhodes and J. Fang, *ACS Omega* 2020, **5**, 18198–18204.

22. W. Liang, S. He and J. Fang, Langmuir 2014, **30**, 805–811.

23. K. Takechi, K. P. Sudeep and P. V. Kamat, *J. Phys. Chem. B* 2006, **110**, 16169– 16173,

24. O. P. Dimitriev, J. Zirzlmeier, A. Menon,Y. Slominskii and M. G. Dirk M. *J. Phys. Chem. C* 2021, **125**, 9855–9865.

25. R. F. Khairutdinov and N. Serpone, *J. Phys. Chem. B* 1997, **101**, 2602–2610.

26. R. Tempelaar, T. L. C. Jansen and J. Knoester, *J. Phys. Chem. Lett.* 2017, **8**, 6113–6117.

27. A. K. Chibisov, A. G. V. Zakharova and H. Görner, *Phys. Chem. Chem. Phys*. 1999, **1**, 1455–1460.

28. N. R. Reddy, S. Rhodes, Y. Ma and J. Fang. *Langmuir* 2020, **36**, 13649–13655

29. V. N. Bliznyuk, S. Kirstein and H. Möhwald, *J. Phys. Chem.* 1993, **97**, 569–574.

30. Z. Li, S. Mukhopadhyay, S. H. Jang, J. L. Bredas and A. K. Y. Jen, *J. Am. Chem. Soc*. 2015, **137**, 11920−11923.

31. A. Klegeris, L. G. Korkina and S. G. Greenfield, *Free Radical Biol. Med.* 1995, **18**, 215–222.

32. X. Ji, G. Palui, T. Avellini, H. B. Na, C. Yi, K. L. Knappenberger and H. Mattoussi, *J. Am. Chem. Soc*. 2012, **134**, 6006–6017.

33. B. Mizrahi, S. A. Shankarappa, J. M. Hickey, J. C. Dohlman, B. P. Timko, K. A. Whitehead, J.-J. Lee, R. Langer, D. G. Anderson, D. S. Daniel and S. Kohane. *Adv. Funct. Mater*. 2013, **23**, 1527–1533.

34. J. L. Bredas, R. Silbey, D. S. Boudreux and R. R. Chance, *J. Am. Chem. Soc.* 1983, **105**, 6555–6559.

35. H. Mohammad-Shiri, M. Ghaemi, S. Riahi, A. Akbari-Sehat, *Int. J. Electrochem. Sci.* 2011, **6**, 317–336.

36. R. R. Howell and J. B. Wyngaar, *J. Biol. Chem.* 1960, **226**, 3544–3550.

37. R. Filograna, L. Civiero, V. Ferrari, G. Codolo, E. Greggio, L. Bubacco, M. Beltramini, M.; M. Bisaglia, *PLOS One* 2015, 0136769.

38. L.-M. Chen and K. X. Chai, *Oncotarget* 2017, **8**, 56490–56505.

39. R. A. Wise and P. P. Rompre, *Annu. Rev. Psychol.* 1989, **40**, 191–225.

40. V. L. Pidoplichko, M. DeBiasi, J. T. Williams and J. A. Dani, *Nature* 1997, **390**, 401–404.

Figure Captions

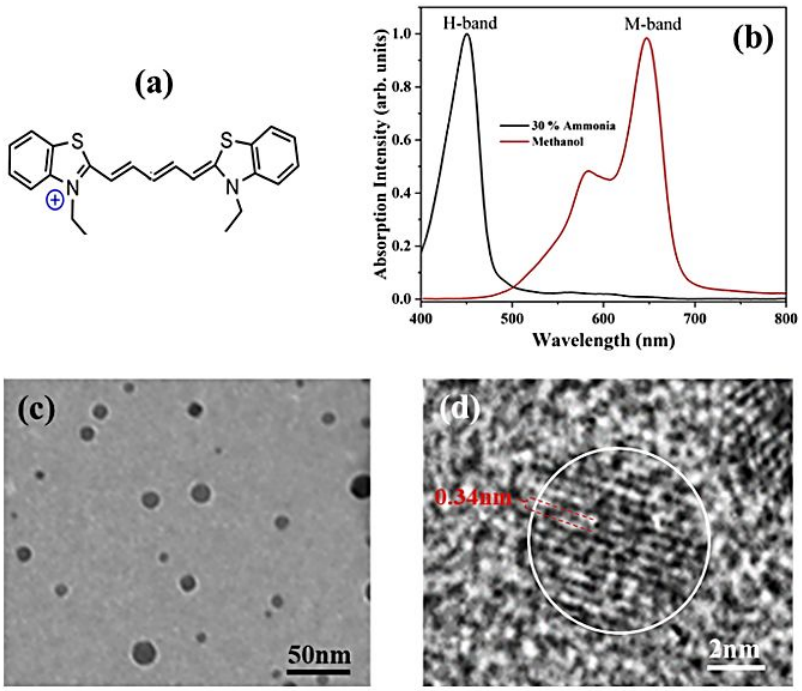

Fig. 1. (a) Chemical structure of $DiSC_2(5)$. (b) UV-vis absorption spectra of 1mM $DiSC_2(5)$ in methanol and 30% ammonia solution. (c) Low and (d) high-resolution TEM images of crystalline H-aggregate nanoparticles of $DiSC_2(5)$ in 30% ammonia solution after being aged for 72h.

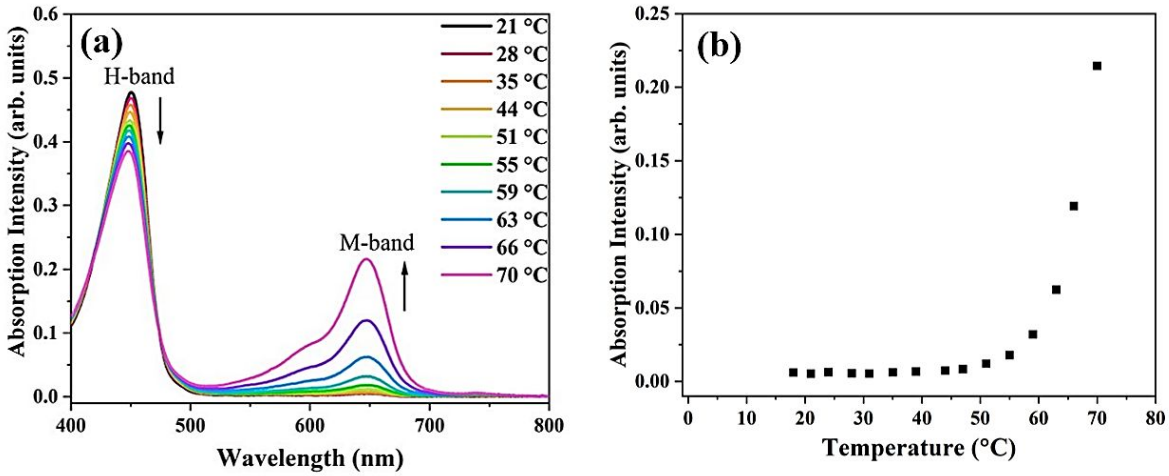

Fig. 2. (a) The temperature-dependent UV-vis absorption spectra of crystalline H-aggregate nanoparticles in ammonia solution after being aged for 72 h. (b) The plot of the M-band intensity as a function of temperature.

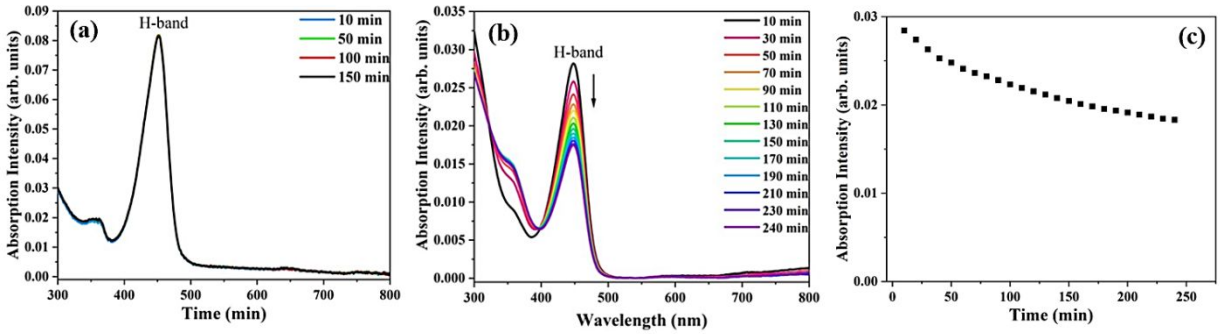

Fig. 3. The time-dependent UV-vis absorption spectra of crystalline H-aggregate nanoparticles in diluted synthetic urine without (a) and with (b) 1μM DA at room temperature. (c) The plot of the H-band intensity as a function of time after the addition of 1μM DA. The crystalline H-aggregate nanoparticles were formed in 30% ammonia solution after being aged for 72 h.

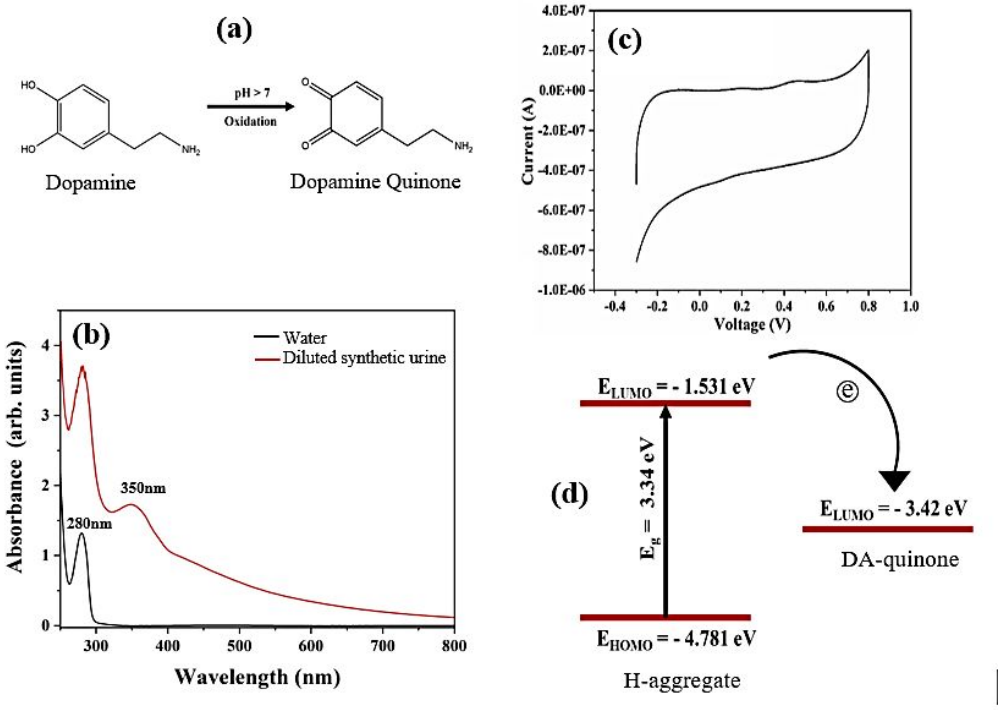

Fig. 4. (a) Schematic representation of DA oxidation in aqueous solution. (b) UV-vis absorption spectra of 0.5 μM DA in water and diluted synthetic urine. (c) Cyclic voltammogram of crystalline H-aggregate nanoparticles. (d) Schematic energy band diagram of crystalline H-

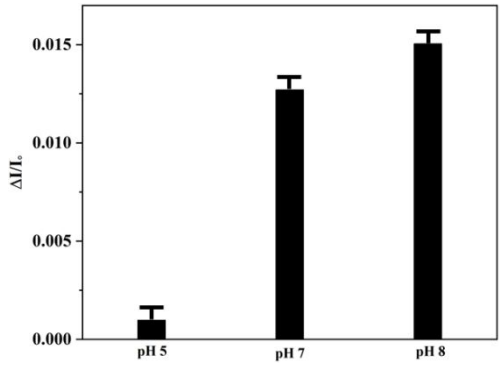

Fig. 5. The relative intensity change ($\Delta I/I_0$) of the H-band of crystalline H-aggregate nanoparticles in buffer solution with pH 5, 7, and 8 upon the addition of 20 nM DA. The H-band intensity change was measured after 240 min incubation of crystalline H-aggregate nanoparticles with DA in buffer solution.

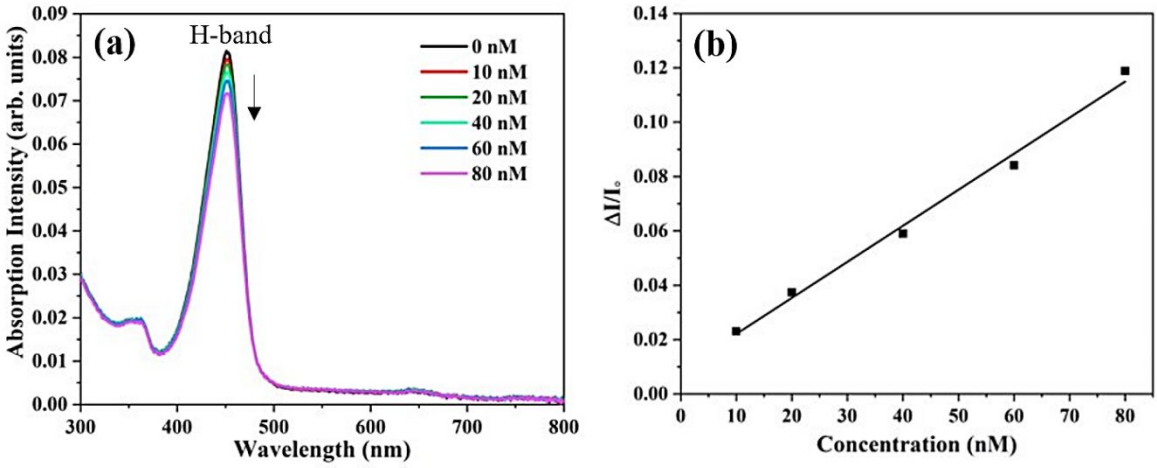

Fig. 6. (a) UV-vis absorption spectra of crystalline H-aggregate nanoparticles in diluted synthetic urine after the addition of DA with the concentration from 10 nM to 80 nM. (b) The plot of the relative intensity change ($\Delta I/I_0$) of the H-band as a function of DA concentrations. The crystalline H-aggregate nanoparticles were formed in 30% ammonia solution after being aged for 72 h. Each spectrum was taken after 240 min incubation with DA.

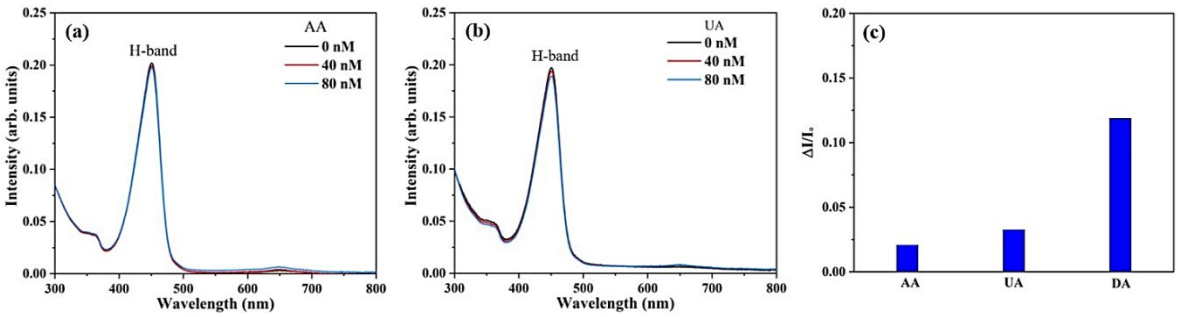

Fig. 7. UV-vis absorption spectra of crystalline H-aggregate nanoparticles in diluted synthetic urine after the addition of AA (a) and UA (b) with the concentration from 10 nM to 80 nM. (c) The plot of the relative intensity change ($\Delta I/I_0$) of the H-band at 80 nM AA, UA, and DA. The crystalline H-aggregate nanoparticles were formed after being aged for 72h in 30% ammonia solution. Each spectrum was taken after 240 min incubation with AA (a) and UA (b).

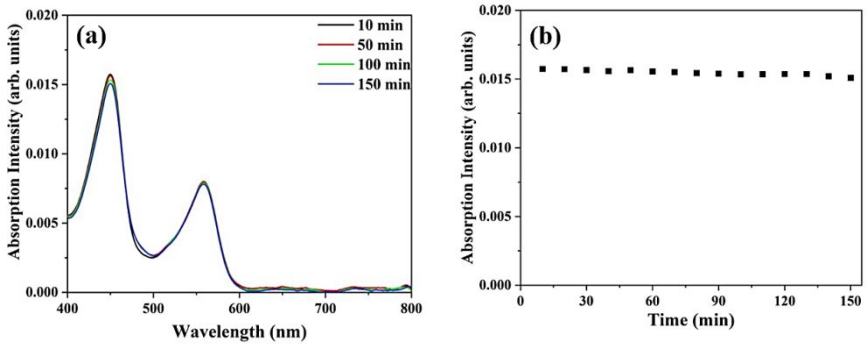

Fig. 8. (a) The time-dependent UV-vis absorption spectra of crystalline H-aggregate nanoparticles in diluted culture medium. (b) The plot of the H-band intensity as a function of time. The crystalline H-aggregate nanoparticles were formed after being aged for 72h in 30% ammonia solution.

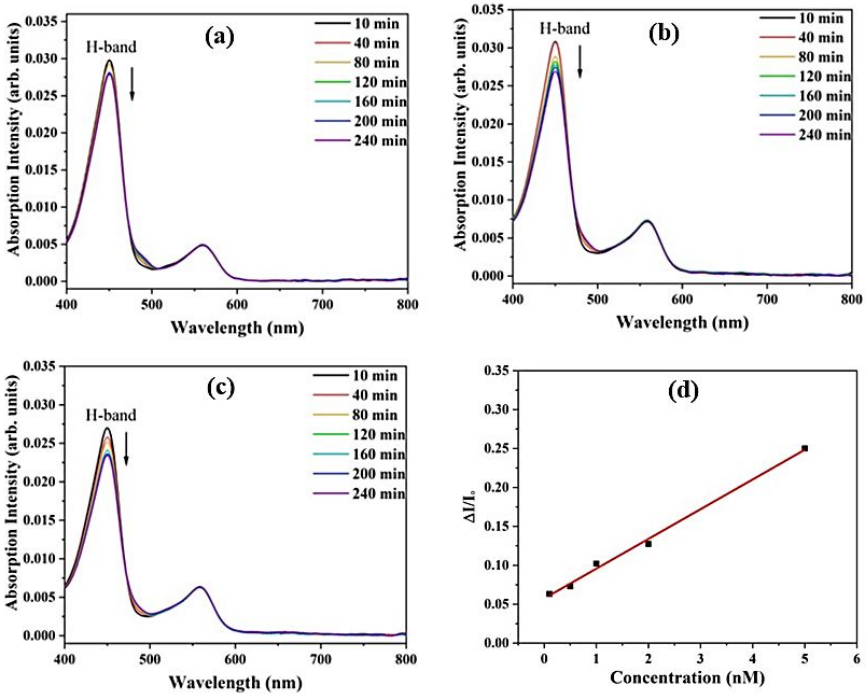

Fig. 9. UV-vis absorption spectra of crystalline H-aggregate nanoparticles in diluted culture medium after the addition of 0.1 nM (a), 1 nM (b), and 2 nM (c) DA. (d) The plot of the relative intensity change ($\Delta I/I_O$) of the H-band as a function of DA concentrations. The crystalline H-aggregate nanoparticles were formed after being aged for 72h in 30% ammonia solution.

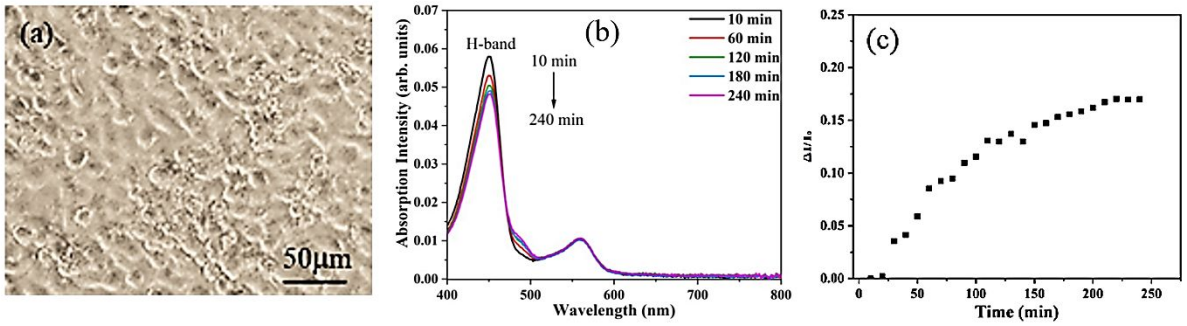

Fig. 10. (a) Phase contrast microscopy image of M17 cells cultured on the 12-well plate. (b) Time-dependent UV-vis absorption spectra of crystalline H-aggregate nanoparticles in the diluted culture medium of M17 cells without nicotine stimulation. (c) Relative intensity change ($\Delta I/I_o$) of the H-band at 450 nm as a function of time. The crystalline H-aggregate nanoparticles were formed after being aged for 72h in 30% ammonia solution.

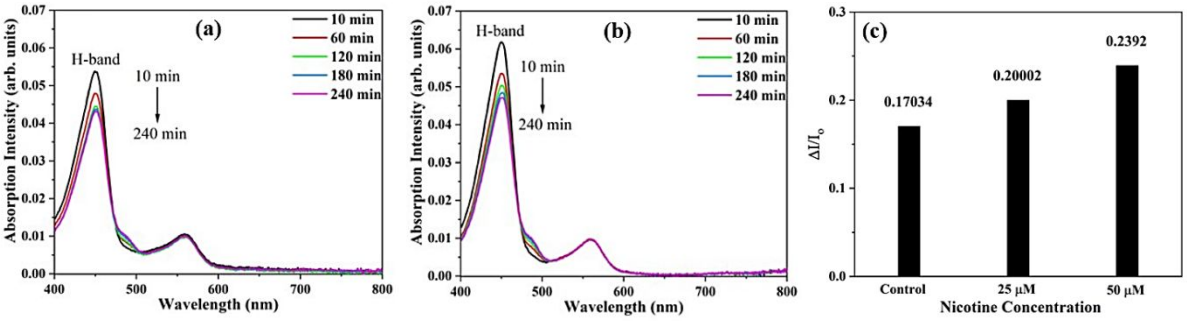

Fig. 11. Time-dependent UV-vis absorption spectra of crystalline H-aggregate nanoparticles in the diluted culture medium of M17 cells with 25 μM (a) and 50 μM (b) nicotine stimulations. (c) The relative intensity change ($\Delta I/I_o$) of H-band at 450 nm after 240 min incubation with 0 μM, 25 μM, and 50 μM nicotine. The crystalline H-aggregate nanoparticles were formed after being aged for 72 h in 30% ammonia solution.